

together impact on the RCu initially formed from metathesis. The precise nature of the reagent, which clearly must involve halide ion (as in, e.g., **2**) along with an assist from the Lewis acid, cannot, however, be identified with certainty at this time.

Acknowledgment. Financial support provided by the NSF and by the donors of the Petroleum Research Fund, administered by the American Chemical Society, is gratefully acknowledged.

Registry No. MeLi, 917-54-4; CuI, 7681-65-4; Lil, 10377-51-2; BF₃, 7637-07-2.

Electronic Structure of Peroxide-Bridged Copper Dimers of Relevance to Oxyhemocyanin

Paul K. Ross and Edward I. Solomon*

Department of Chemistry, Stanford University
Stanford, California 94305

Received February 26, 1990

The active site of oxyhemocyanin (oxyHc) consists of two tetragonal Cu(II) ions separated by ~ 3.6 Å and exhibits a unique absorption spectrum with an intense band at 580 nm ($\epsilon \sim 1000$ M⁻¹ cm⁻¹) and an extremely intense band at 345 nm ($\epsilon \sim 20000$ M⁻¹ cm⁻¹).¹ These bands have been interpreted as peroxide to Cu(II) charge-transfer transitions from the out-of-plane peroxide Π^*_v and in-plane Π^*_σ orbitals, respectively,² where the 12000-cm⁻¹ Π^*_v - Π^*_σ splitting is much larger than the 4000-cm⁻¹ splitting observed for peroxide bound to a single Cu(II).³ On the basis of studies of oxyHc and the met azide derivative,⁴ a spectroscopically effective model^{2,5} of oxyHc has been developed in which the two coppers are bridged by peroxide in an end-on *cis-μ-1,2* fashion and by a second endogenous ligand, likely hydroxide, **1** in Figure 1. However, the recent structural characterization of the first side-on $\mu-\eta^2:\eta^2$ peroxide-bridged transition-metal dimer,⁶ **2**, provides an alternative possibility for the active site of oxyHc. We report here the results of electronic structure calculations on peroxide-bridged copper dimers with geometries **1** and **2**. We have found that the primary bonding interaction in both dimer systems involves the peroxide Π^*_σ with the antisymmetric combination of Cu d_{xy} orbitals which form the LUMO. In addition, the unoccupied peroxide σ^* orbital of **2** acts as a π acceptor influencing the bonding properties of this complex.

Broken-symmetry, spin-unrestricted SCF-X α -Scattered Wave (SCF-X α -SW) calculations⁷ were performed on **1** with an end-on *cis-μ-1,2* bridging geometry⁸ and an effective C_{2v} symmetry and **2** with a side-on $\mu-\eta^2:\eta^2$ bridging geometry⁹ and an effective D_{2h} symmetry. The symmetries were lowered to C_s and C_{2v} by using

* Author to whom all inquiries should be addressed.

(1) (a) Solomon, E. I.; Penfield, K. W.; Wilcox, D. E. *Struct. Bonding (Berlin)* **1983**, *53*, 1-57. (b) Solomon, E. I. *Pure Appl. Chem.* **1983**, *55*, 1069-1088. (c) Solomon, E. I. In *Copper Proteins*; Spiro, T. G., Ed.; Wiley: New York, 1981; pp 41-108.

(2) Eickman, N. C.; Himmelwright, R. S.; Solomon, E. I. *Proc. Natl. Acad. Sci. U.S.A.* **1979**, *76*, 2094-2098.

(3) Pate, J. E.; Cruse, R. W.; Karlin, K. D.; Solomon, E. I. *J. Am. Chem. Soc.* **1987**, *109*, 2624-2630.

(4) Pate, J. E.; Ross, P. K.; Thamann, T. J.; Reed, C. A.; Karlin, K. D.; Sorrel, T. N.; Solomon, E. I. *J. Am. Chem. Soc.* **1989**, *111*, 5198-5209.

(5) Solomon, E. I. In *Metal Clusters in Proteins*; Que, L., Jr., Ed.; ACS Symposium Series 372; American Chemical Society: Washington, DC, 1988; pp 116-149.

(6) Kitajima, N.; Fujisama, K.; Moro-oka, Y.; Toriumi, K. *J. Am. Chem. Soc.* **1989**, *111*, 8975-8976.

(7) (a) Slater, J. C. *Adv. Quantum Chem.* **1972**, *6*, 1-92. (b) Johnson, K. H. *Ibid.* **1973**, *7*, 143-185. (c) Case, D. A. *Annu. Rev. Phys. Chem.* **1982**, *33*, 151-171.

(8) Geometric parameters: Cu-Cu = 3.60 Å, Cu-O = 2.00 Å, O-O = 1.44 Å, Cu-N = 2.00 Å, N-H = 1.00 Å, and \angle Cu-O-O = 122.7°. Sphere radii: $r(\text{Cu}) = 2.95$ bohr, $r(\text{O}) = 1.84$ bohr, $r(\text{N}) = 1.70$ bohr, and $r(\text{H}) = 1.17$ bohr.

(9) Geometric parameters: Cu-Cu = 3.56 Å, Cu-O = 1.90 Å, O-O = 1.42 Å, Cu-N = 2.00 Å, and N-H = 1.00 Å. Sphere radii: $r(\text{Cu}) = 2.70$ bohr, $r(\text{O}) = 1.75$ bohr, $r(\text{N}) = 1.70$ bohr, and $r(\text{H}) = 1.17$ bohr.

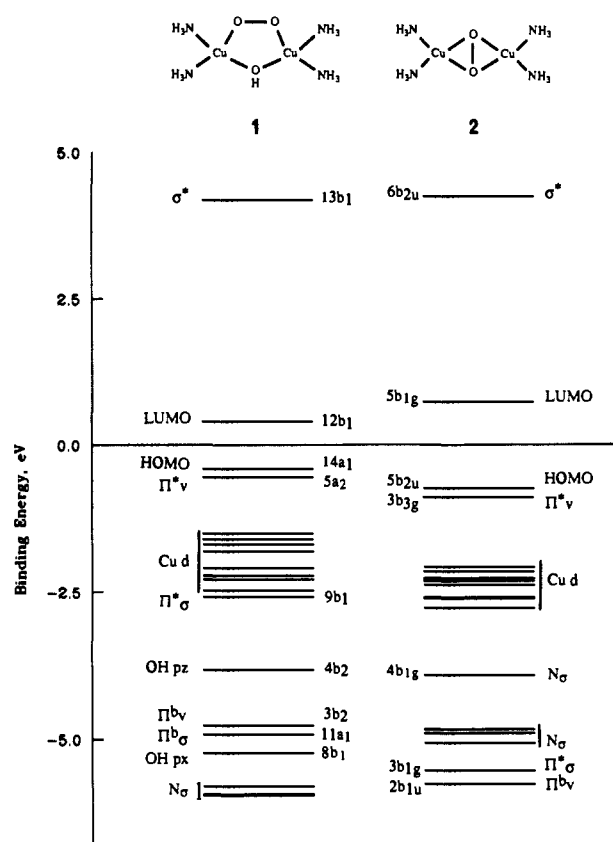


Figure 1. Energy level diagrams of **1**, end-on *cis-μ-1,2*-peroxo (left), and **2**, side-on $\mu-\eta^2:\eta^2$ -peroxo (right). The energy scale has been linearly shifted such that 0 eV is centered between the HOMO and LUMO and energy levels have been labeled by using the full symmetry designations.

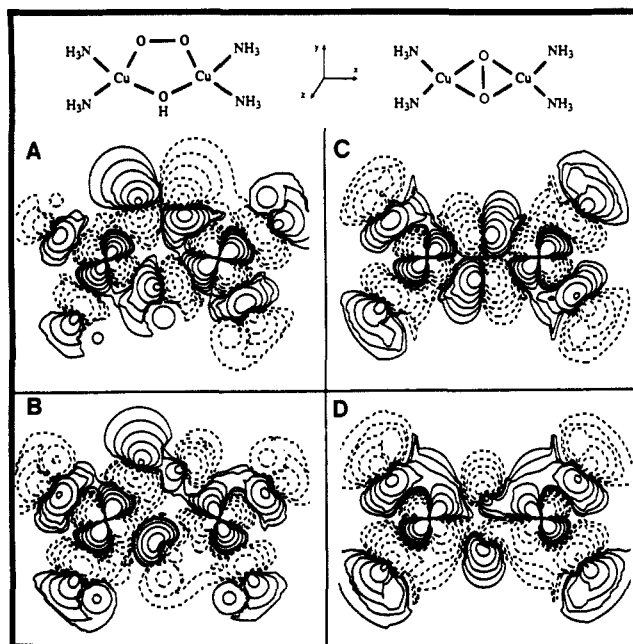


Figure 2. Contour plots of the partially localized broken-symmetry wave functions in the xy plane for (A) spin-up level $12b_1$ (LUMO) of **1**, (B) spin-up level $14a_1$ (HOMO) of **1**, (C) spin-up level $5b_{1g}$ (LUMO) of **2**, and (D) spin-up level $5b_{2u}$ (HOMO) of **2**. Contours located at ± 0.005 , ± 0.01 , ± 0.02 , ± 0.04 , ± 0.08 , and ± 0.16 (e/bohr)^{3/2}.

the broken-symmetry formalism developed by Noodleman¹⁰ which imposes a mirror up-down spin symmetry on opposite halves of the dimer. As with previous calculations,¹¹ the radii of the spheres

(10) (a) Noodleman, L.; Norman, J. G., Jr. *J. Chem. Phys.* **1979**, *70*, 4903-4906. (b) Noodleman, L. *Ibid.* **1981**, *74*, 5737-5743.

surrounding the copper atoms were increased above the Norman criteria¹² to compensate for the tendency to overestimate covalency effects. The $-2J$ values of the ground-state exchange interaction were calculated by using the strong valence bond coupling limit with large overlap between metals. However, the end-on $\text{cis-}\mu\text{-1,2}$ dimer is probably closer to the weak coupling limit which would give values twice as large as that calculated for the singlet-triplet splitting.^{10,13}

The orbital energy diagram of **1** is shown in Figure 1, left. The dominant copper-peroxide bond stabilizes the peroxide Π^*_σ (relative to Π^*_π) while destabilizing the antisymmetric combination of Cu d_{xy} orbitals which form the LUMO ($12b_1$) shown in Figure 2A. The HOMO ($14a_1$) shown in Figure 2B is the symmetric combination of Cu d_{xy} orbitals and is also slightly destabilized due to a weak antibonding interaction with the peroxide Π^*_σ ($11a_1$). The bridging hydroxide p_x provides an additional significant destabilizing interaction on the LUMO which combines with the peroxide Π^*_σ in Figure 2A to increase the HOMO-LUMO splitting. This splitting results in a large calculated ground-state exchange interaction of $-2J = 1850 \text{ cm}^{-1}$.¹⁴

Broken-symmetry SCF- $X\alpha$ -SW calculations on **2** produce the orbital energy diagram in Figure 1, right. The dominant copper-peroxide bonding interaction again involves the Cu d_{xy} and peroxide Π^*_σ resulting in a large stabilization of the Π^*_σ ($3b_{1g}$) while destabilizing the antisymmetric combination of Cu d_{xy} orbitals which form the LUMO ($5b_{1g}$) shown in Figure 2C. Due to the larger orbital overlap of both oxygens with the d_{xy} orbitals on each copper, this bonding interaction stabilizes the Π^*_σ to a much deeper energy than in the end-on case, **1**. In addition, the Cu d_{xy} HOMO ($5b_{2u}$) shown in Figure 2D is stabilized due to a bonding interaction with the unoccupied peroxide σ^* ($6b_{2u}$). *To our knowledge this is the first observation of the peroxide σ^* acting as a π acceptor orbital.* The Π^*_σ donor and σ^* acceptor interactions both increase the HOMO-LUMO splitting which is larger than in **1** and has a correspondingly larger ground-state exchange interaction calculated to be $-2J = 5660 \text{ cm}^{-1}$.¹³

Comparison of the two structures indicates that the dominant bonding interaction in both involves stabilization of the Π^*_σ with the side-on dimer having a larger stabilization and an additional π accepting interaction with the σ^* orbital. This leads to a more stable peroxide-copper bond and a larger HOMO-LUMO splitting and thus a larger exchange interaction for the side-on structure **2**. The charge on the peroxide is found to be less negative in **2** due to the stronger Π^*_σ donor interaction;¹⁵ however, the additional σ^* acceptor interaction in **2** shifts a small amount of electron density into a strongly antibonding MO. This provides a direct explanation for the low O-O stretching frequency observed in the Raman spectrum of this model complex¹⁶ and possibly of oxyHc.¹⁷ The Π^*_σ of **1** is significantly stabilized with respect to the Π^*_π by 16500 cm^{-1} and is consistent with the large observed

$\Pi^*_\nu\text{-}\Pi^*_\sigma$ splitting of oxyHc. The side-on dimer, **2**, has an even larger $\Pi^*_\nu\text{-}\Pi^*_\sigma$ splitting resulting in the Π^*_σ level being deeper in energy, below the $N_\sigma\text{-Cu}$ bonding levels.¹⁸ Significant mixing between the peroxide Π^*_σ ($3b_{1g}$) and the N_σ ($4b_{1g}$) occurs, destabilizing the N_σ level by $\sim 9000 \text{ cm}^{-1}$, resulting in a $\Pi^*_\nu\text{-}N_\sigma$ ($+\Pi^*_\sigma$) splitting of 25000 cm^{-1} . This would lead to an alternative possible assignment of the higher energy charge-transfer band in oxyHc based on **2** as a $N_\sigma \rightarrow \text{Cu}$ charge transfer which has been lowered in energy due to a large peroxide Π^*_σ mixing. This assignment would provide insight into the UV resonance Raman excitation profiles of oxyHc which exhibit dominant enhancement of Cu-N modes.¹⁷ However, we have found experimentally that the Π^*_σ transition in an end-on $\text{trans-}\mu\text{-1,2}$ bridging model complex¹⁹ also exhibits this unusual resonance enhancement.²⁰ These calculations indicate that both structures are viable models for oxyHc, with the side-on dimer providing insight into the vibrational data and the end-on dimer a more direct assignment of the oxyHc charge-transfer spectrum. Single-crystal absorption experiments on oxyHc should distinguish between the two bridging geometries based on the differences in D_{2h} and C_{2v} selection rules of the peroxide charge-transfer transitions.

Acknowledgment. We thank Dr. Michael Cook for useful discussions and the NIH for funding (AM31450).

(18) While Hc has histidine and the model complex **2** involves pyrazolyl ligation, we have found the σ bonding interactions of imidazole to be well modeled by NH_3 . Penfield, K. W.; Gewirth, A. A.; Solomon, E. I. *J. Am. Chem. Soc.* **1985**, *107*, 4519-4529.

(19) Jacobson, R. R.; Tyeklar, Z.; Farooq, A.; Karlin, K. D.; Liu, S.; Zubieta, J. *J. Am. Chem. Soc.* **1988**, *110*, 3690-3692.

(20) Baldwin, M. J.; Ross, P. K.; Karlin, K. D.; Solomon, E. I., manuscript in preparation.

Nonexistence of Dianionic Pentacovalent Intermediates in an *ab Initio* Study of the Base-Catalyzed Hydrolysis of Ethylene Phosphate[†]

Carmay Lim and Martin Karplus*

Department of Chemistry, Harvard University
12 Oxford Street, Cambridge, Massachusetts 02138

Received February 22, 1990

Phosphorus has a broad role in living systems,¹ and the reactions of phosphate esters in solution and in enzymes are of great interest. Pentacovalent phosphorus intermediates or transition states that are formed by nucleophilic attack on the tetracoordinated phosphorus atom^{2,3} have been postulated in the nonenzymatic hydrolysis of cyclic and open-chain phosphinates, phosphonates, and phosphates,⁴ as well as in the enzymatic hydrolysis of cyclic phosphates.⁵ Such intermediates have not been isolated, although there is evidence for pentavalency from ³¹P chemical shift measurements.⁶ A pentacovalent intermediate explains⁷ that the acid-catalyzed hydrolysis of hydrogen or methyl ethylene phosphate in water enriched in ¹⁸O is accompanied by exchange of ¹⁸O into the unreacted ester.^{8,9} This exocyclic cleavage with ring

(11) (a) Gewirth, A. A.; Cohen, S. L.; Schugar, H. J.; Solomon, E. I. *Inorg. Chem.* **1987**, *26*, 1133-1146. (b) Didziulis, S. V.; Cohen, S. L.; Gewirth, A. A.; Solomon, E. I. *J. Am. Chem. Soc.* **1988**, *110*, 250-268. (c) Gewirth, A. A.; Solomon, E. I. *J. Am. Chem. Soc.* **1988**, *110*, 3811-3819.

(12) (a) Norman, J. G., Jr. *J. Chem. Phys.* **1974**, *61*, 4630-4635. (b) Norman, J. G., Jr. *Mol. Phys.* **1976**, *31*, 1191-1198.

(13) Very large $-2J$ values have been calculated for strongly coupled copper dimers. Bencini, A. *J. Chim. Phys. Phys.-Chim. Biol.* **1989**, *86*, 763-787.

(14) Broken-symmetry $X\alpha$ calculations of $-2J$ exchange coupling values are often found to be too high by a factor of 2. (a) Noodleman, L.; Baerends, E. J. *J. Am. Chem. Soc.* **1984**, *106*, 2316-2327. (b) Noodleman, L.; Case, D. A.; Sontum, S. F. *J. Chim. Phys. Phys.-Chim. Biol.* **1989**, *86*, 743-755. (c) Sontum, S. F.; Noodleman, L.; Case, D. A. In *The Challenge of d and f Electrons: Theory and Computation*; Salahub, D. R., Zerner, M. C., Eds.; ACS Symposium Series 394; American Chemical Society: Washington, DC, 1989; pp 366-377.

(15) The effective charge on the peroxide based on the relative values of the self-consistent potential near the oxygen nucleus was estimated to be -2.09 for **1** and -1.63 for **2**. Case, D. A.; Huynh, B. A.; Karplus, M. *J. Am. Chem. Soc.* **1979**, *101*, 4433-4453.

(16) Kitajima, N.; Koda, T.; Hashimoto, S.; Kitagawa, T.; Moro-oka, Y. *J. Chem. Soc., Chem. Commun.* **1988**, 151-152.

(17) (a) Larrabee, J. A.; Spiro, T. G. *J. Am. Chem. Soc.* **1980**, *102*, 4217-4223. (b) Freedman, T. B.; Loehr, J. S.; Loehr, T. M. *Ibid.* **1976**, *98*, 2809-2815.

[†]This work was supported in part by a grant from the NSF.

(1) Westheimer, F. H. *Science* **1987**, *237*, 1173.

(2) Hudson, R. F.; Brown, C. *Acc. Chem. Res.* **1972**, *5*, 204.

(3) Emsley, J.; Hall, D. *The Chemistry of Phosphorus*; John Wiley and Sons: New York, 1976.

(4) Cox, J. R., Jr.; Ramsay, B. *Chem. Rev.* **1964**, *64*, 317.

(5) Fersht, A. *Enzyme Structure and Mechanism*; W. H. Freeman: New York, 1985.

(6) Allen, D. W.; Hutley, B. G.; Mellor, M. T. *J. Chem. Soc. Perkin Trans. II* **1972**, 63.

(7) Westheimer, F. H. *Acc. Chem. Res.* **1968**, *1*, 70.

(8) Haake, P. C.; Westheimer, F. H. *J. Am. Chem. Soc.* **1961**, *83*, 1102.